BNL-NUREG-23709
INFORMAL REPORT

SPATIAL WEIGHTING OF DOPPLER REACTIVITY FEEDBACK

JOHN F. CAREW
DAVID J. DIAMOND
MICHAEL TODOSOW

THERMAL REACTOR SAFETY DIVISION

DATE PUBLISHED

DECEMBER 1977

DEPARTMENT OF NUCLEAR ENERGY BROOKHAVEN NATIONAL LABORATORY
UPTON, NEW YORK 11973

Prepared for the U.S. Nuclear Regulatory Commission
Office of Nuclear Reactor Regulation
Contract No. EY-76-C-02-0016

BNL-NUREG-23709
INFORMAL REPORT
UNLIMITED DISTRUBUTION

SPATIAL WEIGHTING OF DOPPLER REACTIVITY FEEDBACK

John F. Carew
David J. Diamond
Michael Todosow

REACTOR CORE SAFETY ANALYSIS GROUP
THERMAL REACTOR SAFETY DIVISION
DEPARTMENT OF NUCLEAR ENERGY
BROOKHAVEN NATIONAL LABORATORY
UPTON, NEW YORK 11973

December 1977

Available from
National Technical Information Service
U.S. Department of Commerce
5285 Port Royal Road
Springfield, VA 22161

ABSTRACT

The spatial weighting of the local Doppler feedback implicit in the determination of the core Doppler feedback reactivity has been investigated. Using a detailed planar PDQ7-II PWR model with local fuel-temperature feedback, the core Doppler spatial weight factor, S, has been determined for various control patterns and power levels. Assuming power-squared weighting of the local Doppler feedback, a simple analytic expression for S has been derived and, based on comparison with the PDQ7-II results, provides a convenient and accurate representation of the Doppler spatial weight factor. The sensitivity of these results to variations in the fuel rod heat transfer coefficients, fuel loading and the magnitude of the Doppler coefficient has also been evaluated. The dependence of the local Doppler coefficient on moderator temperature, boron concentration and control rod density has been determined and found to be weak. Selected comparisons with vendor analyses have been made and indicate general agreement.

Table of Contents

List of Tables

List of Tables (Cont'd.)

List of Figures

I. INTRODUCTION

The calculation of Doppler feedback is generally separated into a pin-cell Doppler coefficient based on the temperature dependent resonance integral calculation and the calculation of a Doppler spatial weight factor, S. The spatial weight factor, S, accounts for the flux weighting of the Doppler feedback and the distribution of the change in fuel temperature and is introduced in order to uncouple the Doppler feedback from the point or one-dimensional transient analysis. In the present study the determination of the spatial weight factor will be considered while the Doppler resonance integral calculation will be addressed in Reference 1.

The following types of Doppler weighting occur: (1) core-weighting, an increase in feedback ($S^C > 1.0$) due to the core temperature distribution[2] and (2) pin-weighting, a decrease in feedback ($S^P < 1.0$) due to the local pin temperature distribution.[3] In addition, although not due to spatial weighting, the Doppler feedback is reduced as a result of lattice weighting ($S^L < 1.0$) due to the binding of the U-238 atoms in the crystal lattice.[4] The core-weighting results from the relatively large fuel temperature changes that occur in the high powered and therefore high weight assemblies. The pin-weighting results from the relatively small fuel temperature changes that occur near the pin surface, where a larger fraction of the absorptions take place and where the neutron importance is high. The decrease in Doppler feedback in a

crystal lattice results from (1) the reduction in fuel temperature change due to crystal binding and (2) the increase in effective fuel temperature and broadening of the U-238 resonances.

At operating temperatures the feedback reduction due to lattice binding is of the order of a percent[5] and the pin-weighting effect is small (see, Appendix-B). The core-Doppler-weighting will be the subject of the present evaluation.

Sha[6] has made an experimental determination of the core Doppler weight factor using an empirical correlation of measured (Doppler-only) power coefficients for three Westinghouse PWR's. Poncelet[7] has used a semi-empirical method to determine the core-Doppler weighting using measured core flux distributions to weight the calculated local Doppler perturbation.

Calculations of the core-Doppler weighting are generally based on the adiabatic approximation[8] in which the Doppler reactivity is determined from three-dimensional or planar neutronics calculations by eigenvalue differencing. These calculations generally result in a generic correlation of Doppler weight factor versus core power peaking-factor.[9,10] In some cases S^{core} is determined for specific accidents via a conservative normalization of point kinetics calculations to multidimensional transient analyses by adjustment of S^{core}. This method has the disadvantage that S^{core} will in principle depend on the accident being analyzed.

The purpose of the present analysis is twofold. First, to perform a simplified analytic analysis of the Doppler spatial weighting which will exhibit the important dependencies on the fuel temperature distribution and feedback mechanism and which can be extended to more general feedback situations of interest. And second, to perform neutronics calculations to determine in detail the assembly and core Doppler-fuel temperature response and hence to provide a benchmark for the simplified analytic analysis. In addition, a general evaluation of PWR Doppler reactivity calculations, including comparisons with vendor results, will be made.

The simplification made in the analytic treatment is based on the following two assumptions: (1) the weighting of the local Doppler feedback is to a good approximation a power-squared, $P^2(\underline{x})$, weighting and (2) the spatial dependence of the local feedback enters only through the power, $P(\underline{x})$. This allows the spatial integral defining the core Doppler feedback to be transformed to an integral over power and expressed in terms of the low-order central moments of the assembly-wise power frequency distribution.

The numerical calculations were performed for a (Westinghouse, RESAR-3) PWR core using the programs HAMMER,[11] TWOTRAN-II[12] and PDQ7-II.[13] The local Doppler feedback was included in the PDQ7-II calculations using cross sections which were interpolated locally on fuel temperature. In both the analytic and numerical analysis the

spatial weighting factors were determined by eigenvalue differencing based on the adiabatic approximation.

In Section II the temperature-distribution and flux-distribution spatial weighting factors are defined and in Section III the calculational model and its qualification are presented. The analytical and numerical analysis of the temperature-distribution weight factor is presented in Section IV. In Section V the flux-distribution weight factor is determined and the results and conclusions are summarized in Section VI.

II. SPATIAL WEIGHTING OF DOPPLER FEEDBACK

The point kinetics reactivity for a state defined by the flux vector - ϕ is defined by the relation,

$$\rho(t) = \langle W, (\mathcal{P}-\mathcal{D})\phi(t) \rangle / \langle W, \mathcal{P}(t) \rangle$$

$$= \langle W, \mathcal{P}_N \phi(t) \rangle / \langle W, \mathcal{P}\phi(t) \rangle \qquad (1)$$

The production ($\mathcal{P}$) and destruction ($\mathcal{D}$) operators are defined (in the standard notation) by

$$\mathcal{P}_{gg'}(t) = \sum_j \left[(1-\beta^j)\chi^j_{pg} + \sum_{i=1}^{6} \beta^j_i \chi_{ig}\right] \nu^j \quad \Sigma^j_{Fg'}$$

$$\mathcal{D}_{gg'}(t) = -\underline{\nabla} \cdot D_g \underline{\nabla} \delta_{gg'} + \quad \Sigma_{T\,gg'} \qquad (2)$$

and the net production operator is,

$$\mathcal{P}_N = \mathcal{P} - \mathcal{D}. \qquad (3)$$

ϕ is the 3-dimensional transient perturbed solution and W is a conveniently chosen weighting function.

At time t, the steady-state or adiabatic flux solution is defined by the equation,

$$\mathcal{P}(t)\ \phi_A = k\mathcal{D}(t)\ \phi_A \qquad (4)$$

where k is the steady-state eigenvalue. If in equation (1) ϕ is approximated by ϕ_A , the adiabatic-approximation results,

$$\rho_A(t) = \langle W, (\mathcal{P}-\mathcal{D})\phi_A(t) \rangle / \langle W, \mathcal{P}\phi_A(t) \rangle$$
$$= 1 - \frac{1}{k} \tag{5}$$

Throughout the present analysis the adiabatic-approximation will be made and the Doppler reactivity and weight factors evaluated using Eq. (5). Although this approximation is known to be inaccurate during certain transients,[8] it is believed sufficiently accurate for taking reactivity ratios as required in the determination of S.

In determining Doppler reactivity it is convenient to separate the spatial effects associated with (1) the flux weighting of the local reactivity response for a given change in temperature and (2) the core temperature distribution, by the introduction of spatial weight factors. This may be accomplished by first defining an isothermal reactivity, ρ_I , for a uniform base core-wide fuel temperature, $\bar{T}$, and reference state, ϕ_1 ,

$$\rho_I(\phi_1, \bar{T}) = \langle W, \mathcal{P}_N(\bar{T})\phi_1 \rangle / \langle W, \mathcal{P}(\bar{T})\phi_1 \rangle \tag{6}$$

A flux-distribution weight factor, S_F , is introduced to relate this base reactivity to the reactivity for the flux of interest, ϕ_2 ,

$$\rho_I(\phi_2, \bar{T}) = S_{F21}(\bar{T})\ \rho_I(\phi_1, \bar{T}) \tag{7}$$

A temperature-distribution weight factor, S_T, is then defined to relate the isothermal reactivity to the reactivity for the case where the fuel temperature varies spatially,

$$\rho(\phi_2, T(\underline{x})) = S_T(\phi_2, T(\underline{x}))\rho_I(\phi_2, \bar{T}) \tag{8}$$

In practice, the normalization of S_T to the isothermal temperature $\bar{T}$ is somewhat arbitrary provided the isothermal reactivity employed in the transient calculation is consistent with that defined for the spatial weight factor, S_T. The isothermal fuel temperature, $\bar{T}$, is therefore a dummy variable used to tabulate reactivity and for convenience will be taken to be the fuel pin temperature at the core-average power $\bar{P}$,

$$\bar{T} = T(\bar{P}), \tag{9}$$

where T(P) defines the pin fuel temperature to power correlation.*

In the typical adiabatic reactivity calculation the reactivity perturbation is introduced by an increase in core power, maintaining the overall power distribution,† $\Delta P \propto P$. In this case, the high (low) powered nodes receive the largest (smallest) temperature change, and therefore the change in local Doppler reactivity, and the spatial weighting are positively correlated and $S > 1.0$. This perturbation is physically reasonable for most transients. In Appendix A the more general case, where the change in power may be expressed as a polynomial in power, $\Delta P \propto P^n$, is treated.

---

*An alternate definition is the core volume-averaged fuel temperature $\bar{T} = \langle T(P(x)) \rangle$. Since T is essentially a linear function of power in the region of interest these definitions agree to within $\sim$ 1%.

†Except for second order power readjustments introduced by local feedback.

III. CALCULATIONAL MODEL

A. Model Description

A planar two-dimensional PDQ7-II diffusion theory model of the Westinghouse RESAR-3 core[14] was constructed for analysis of the Doppler feedback spatial weighting factors.

The RESAR-3 core consists of 193 (2.1, 2.6 and 3.1 w/o enriched) axially homogeneous fuel assemblies. The 2.1 and 2.6 w/o assemblies are arranged in a checkerboard pattern in the central region of the core and the higher 3.1 w/o enrichment assemblies are located on the periphery as shown in Fig. 1. Each assembly consists of 289 rod locations arranged in a 17 x 17 lattice: 2.1 w/o - 264 fuel rods, 24 control rods and instrumentation sheath, 2.6 w/o - 264 fuel rods, 9-20 boron poison rods and instrumentation sheath and 3.1 w/o - 264 fuel rods, 9-20 boron poison rods and instrumentation sheath. In Figures 2-4 a detailed description of the assembly and core laydown is given and in Table I the core and fuel characteristics are presented.

The nuclear cross sections for the PDQ7-II model were determined in two steps. First, homogenized pin-cell 8 group macroscopic cross sections were obtained using the BNL version of HAMMER. Then, assembly averaged macroscopic two-group cross sections were determined using TWOTRAN-II. The HAMMER and TWOTRAN-II cross sections employed in this analysis were generated in a related study[15] and are described here for completeness.

The base HAMMER pin-cell calculations were performed using a 20 mesh-point cylindrical geometry and ENDF/B-IV cross sections at the base condition:

Fuel temperature - T_F = 1000 ^oK,

Moderator temperature- T_M = 586^oF,

Soluble boron concentration - C_B = 1000 ppm.

Three additional calculations were performed in which each variable was individually perturbed, holding the remaining 2 variables at their unperturbed base values: Case-1 (T_F = 800^o K, T_M = 586^{o}F, C_B = 1000 ppm), Case-2 (T_F = 1000^o K, T_M = 586^o F, C_B = 800 ppm) and Case-3 (T_F = 1000^o K, T_M = 500^o F, C_B = 1000 ppm). Pin-cell calculations were performed for the three fuel enrichments, boron poison pin, control pin and for water-rods. HAMMER slab calculations were performed in order to obtain baffle and reflector cross sections.

The effects of thermal expansion, global buckling and Doppler pin-weighting on the pin-cell Doppler feedback are evaluated in Appendix B and found to be small, ($\lesssim$ 2%). In addition, in order to evaluate the ability of HAMMER to calculate the Doppler coefficient for an isolated rod, a detailed evaluation of the HAMMER U-238 resonance integral and temperature coefficient has been made.[1] It is concluded, the HAMMER ENDF/B-IV calculation of the Doppler fuel temperature coefficient is low relative to that implied by the Hellstrand measured data by $\sim$ 9%. However, the spatial weight factors are insensitive to the magnitude

of the Doppler feedback (see Section IV.B) and the effect of this difference on S is negligible.

TWOTRAN-II assembly calculations were performed for the eleven combinations of enrichment, control and poison loading.* As for the pin-cell calculations, a base case and three perturbed cases were calculated. The homogenized pin cross sections were represented with 3 fast groups and 5 thermal groups. The assemblies were calculated in the S-4 approximation using a 70 x 70 mesh and reflecting boundary conditions. These TWOTRAN-II calculations determined the basic PDQ7-II 2-group assembly-homogenized cross section data.

In order to allow for implicit cross section variation with $\sqrt{T_F}$, T_M and C_B in PDQ7-II the cross section dependence was linearized and incorporated using interpolating tables. In order to provide a Σ-representation which would reproduce the basic TWOTRAN-II cross section variation to within $\lesssim$ 5%,57 interpolating tables were required.

The PDQ7-II calculations were performed in planar geometry with 16 mesh-blocks per assembly and an explicit core baffle. The cross section dependence on fuel temperature was achieved by correlating the fuel temperature to local power and then interpolating the cross section on the Iodine-135 number density (which is proportional to power under the equilibrium conditions used).

---

*The 3.1 w/o assembly containing 19 poison rods and 1 source rod was represented by a 20 poison pin assembly.

The effective fuel rod temperature, T_{eff}, is determined by the pin power (kW/FT) and local heat transfer characteristics (fuel conductivity and gap conductance). In this study the Westinghouse RESAR-3 $T_{eff}(P)$ correlation was determined using the Doppler only power coefficient and fuel temperature coefficient[14] by the relation,

$$\frac{dT_{eff}}{dP} = \frac{\Delta\rho}{\Delta P} \Big/ \frac{\Delta\rho}{\Delta T_{eff}} \tag{10}$$

and the condition $T_{eff}(0) = 586\ ^{o}F$.* The resulting $T_{eff}(P)$ was represented as,

$$T_{eff}(P) = a + bP + cP^2, \tag{11}$$

where $a = 586\ ^{o}F$, $b = 126.01\ ^{o}F/(kW/FT)$ and $c = -.5511\ ^{o}F\ (kW/FT)^{-2}$. This correlation includes the effects of lattice and pin-weighting as well as an empirical normalization of the Westinghouse models to measured power coefficient data.

B. Model Qualification

In order to verify the procedures used in constructing the PDQ7-II model geometry, composite laydown, and Σ-representation, full core planar PDQ7-II/TWOTRAN-II comparisons have been made. The TWOTRAN-II and PDQ7-II calculations are based on the same TWOTRAN-II assembly calculations but the

*It is recognized that a more accurate condition is $T_{eff}(0) = T_m = 557\ ^{o}F$; however, this difference has a negligible effect on this analysis.

Σ-data representation, geometry and material representation are completely independent. The TWOTRAN-II calculations were S_2* and employed 36 mesh blocks/assembly. In Table II the PDQ7-II and TWOTRAN-II results are presented for the all rods out (ARO), Bank-D inserted (BDI), and Bank-C and Bank-D inserted (BCDI) cases. The consistent overprediction of the eigenvalue, k, by PDQ7-II in the base fuel temperature (T_F = 727 ^{o}C) cases results from the inclusion of an axial buckling in the TWOTRAN-II planes which is not included in the PDQ7-II calculations. It is seen in the last row that PDQ7-II tracks the Doppler reactivity change, relative to TWOTRAN-II, to within $\sim$ 5%.

In order to further qualify the PDQ7-II model for the RESAR-3 analysis, the ARO base-case critical boron concentration and moderator coefficient were calculated and in Table III a comparison of the PDQ7-II and RESAR-3[13] results is presented. The results are in generally good agreement and within the expected uncertainty of the RESAR-3 data[14]; $\pm$ 2 pcm/^{o}F on moderator coefficient and $\pm$ 50 ppm for C_B (with depletion).

---

*It is noteworthy that S_4 calculations were also performed and were in good agreement with the S_2 results.

IV. DOPPLER TEMPERATURE-DISTRIBUTION WEIGHTING FACTOR - S_T

A. Analysis

It is convenient in the analysis of the temperature-distribution spatial weighting to express the overall temperature distributed reactivity in terms of the local reactivity response. Taking the initial, unperturbed, steady-state adjoint for the weighting* in equation (1) the overall reactivity is,

$$\rho = \langle \phi_o^+, \mathcal{P}_N \phi \rangle / \langle \phi_o^+, \mathcal{P} \phi \rangle . \tag{12}$$

Making use of the fact that the production operator, $\mathcal{P}$, used in the reactivity normalization, is to an excellent approximation ($\lesssim 1\%$) independent of the fuel temperature, and therefore, $\mathcal{P}_o \simeq \mathcal{P}$, it follows that,

$$\rho = \langle \phi_o^+, \mathcal{P}_{No} \phi \rangle / \langle \phi_o^+, \mathcal{P}_o \phi \rangle + \langle \phi_o^+, \Delta\mathcal{P}_N \phi \rangle / \langle \phi_o^+, \mathcal{P} \phi \rangle$$

$$\rho = \rho_o + \langle \phi_o^+, \Delta\mathcal{P}_N \phi \rangle / \langle \phi_o^+, \mathcal{P} \phi \rangle . \tag{13}$$

The reactivity difference between states corresponding to ϕ and ϕ_o is then,

$$\Delta\rho = \langle \phi_o^+, \Delta\mathcal{P}_N \phi \rangle , \tag{14}$$

---

*It is important to note, the total reactivity determined by the adiabatic approximation is independent of the weight function W.

where for convenience the normalization, $< \phi_o^+, \mathcal{P} \phi >$, has been taken to be unity since S_T is independent of the reactivity normalization.

The fluxes ϕ and ϕ_o^+ may be decomposed spatially as,

$$\phi^g(\underline{x}) = \sum_\alpha \phi_\alpha^1 \ \phi_\alpha^g \ (\underline{x}) \tag{15}$$

$$\phi_o^{\dagger g}(\underline{x}) = \sum_\alpha \phi_{o\alpha}^1 \ \phi_{o\alpha}^{\dagger g} \ (\underline{x}) \tag{16}$$

where $\phi_\alpha^g \ (\underline{x})$ and $\phi_{o\alpha}^{\dagger g} \ (\underline{x})$ are defined over the spatial cell-α by,

$$\phi_\alpha^g \ (\underline{x}) = \begin{cases} \phi^g(x)/\phi_\alpha^1 & \underline{x} \ \varepsilon \ \alpha \\ 0 & \text{otherwise} \end{cases} \tag{17}$$

$$\phi_{o\alpha}^{\dagger g} \ (\underline{x}) = \begin{cases} \phi^{\dagger g}(\underline{x})/\phi_{o\alpha}^1 & \underline{x} \ \varepsilon \ \alpha \\ 0 & \text{otherwise} \end{cases} \tag{18}$$

and,

$$\phi_\alpha^1 = v_\alpha^{-1} \int_{x \ \varepsilon \ \alpha} \phi^1(x) \ dx \tag{19}$$

$$\phi_{o\alpha}^1 = v_\alpha^{-1} \int_{x \ \varepsilon \ \alpha} \phi_o^{\dagger 1} \ (x) \ dx \tag{20}$$

v_α is the volume of cell-α. Note, $\phi_\alpha^1(x)$ and $\phi_\alpha^2(x)$ have the same normalization (ϕ_α^1) in order to preserve the true thermal/fast flux ratio.

Inserting these expressions into Eq. (14),

$$\Delta\rho = \sum_{\substack{\alpha \\ g,g'}} \phi_{o\alpha}^1 \, \phi_\alpha^1 \int_{x \,\varepsilon\, \alpha} d\underline{x} \; \phi_{o\alpha}^{\dagger g}(\underline{x}) \; \Delta P_{Ngg'}(\underline{x}) \; \phi_\alpha^{g'}(\underline{x}) \; . \tag{21}$$

The corresponding cell reactivity is,

$$\Delta\rho_\alpha = \sum_{g,g'} \int_{x \,\varepsilon\, \alpha} d\underline{x} \; \tilde{\phi}_{o\alpha}^{\dagger g}(\underline{x}) \; \Delta P_{Ngg'}(\underline{x}) \; \tilde{\phi}_\alpha^{g'}(\underline{x}) \; / \; \sum_{gg'} \int_{x \,\varepsilon\, \alpha} d\underline{x} \; \tilde{\phi}_{o\alpha}^{\dagger g}(x) \, P_{gg'}(\underline{x}) \; \tilde{\phi}_\alpha^{g'}(\underline{x}) \tag{22}$$

where $\tilde{\phi}_{o\alpha}^{\dagger g}$ and $\tilde{\phi}_\alpha^g$ are the flux solutions for the α-cell and have the same normalization as $\phi_{o\alpha}^{\dagger g}(\underline{x})$ and $\phi_\alpha^g(\underline{x})$ (eqs. (17) and (18)).

The cell calculation of $\tilde{\phi}_\alpha(\underline{x})$ and $\tilde{\phi}_{o\alpha}^\dagger(\underline{x})$ differs from the global calculation of $\phi_\alpha(\underline{x})$ and $\phi_{o\alpha}^\dagger(\underline{x})$ only in the boundary condition imposed on the cell. Assuming the effect of the boundary condition on the flux shapes is small,* the global fluxes may be approximated by the cell fluxes and,

$$\Delta\rho = \sum_\alpha \phi_{o\alpha}^1 \, \phi_\alpha^1 \, \Delta\rho_\alpha P_\alpha \; . \tag{23}$$

*This is generally a good approximation for the interior assemblies and breaks down to some extent for the less important peripheral assemblies.

P_α is the flux averaged α-cell neutron production cross section,

$$P_\alpha = \sum_{gg'} P_{\alpha gg'} = \sum_{gg'} \int_{x \in \alpha} d\underline{x}\, \tilde{\phi}^{\dagger g}_{o\alpha}(\underline{x}) P_{gg'}(\underline{x})\, \tilde{\phi}^{g'}_{\alpha}(\underline{x}) \tag{24}$$

The Doppler reactivity for cell-α is determined by the relation,

$$\Delta\rho_\alpha = \alpha_D(T_\alpha)\, \Delta T_\alpha \propto \frac{\Delta T_\alpha}{\sqrt{T_\alpha}} \tag{25}$$

where T_α and ΔT_α are the local temperature and temperature perturbations (in absolute units) and α_D is the local Doppler coefficient which has the typical $T_\alpha^{-1/2}$ behavior.

It is important to note here that the local Doppler coefficient (α_D) is determined primarily by the U-238 loading and is to a good approximation ($\tilde{<}$ 5%) independent of moderator temperature, control density, boron concentration (see the discussion in Section IV and Tables IV - VI) and burnup[16] and therefore independent of the spatial index - α. In the case of a BWR, the Doppler feedback depends on the local void fraction and α_D depends on α.

The temperature-distribution weight factor S_T may then be expressed,

$$S_T = \sum_\alpha P_{\alpha R} \frac{\Delta T(P_\alpha)}{\sqrt{T}(P_\alpha)} \Big/ \left(\frac{\Delta T}{\sqrt{T}}\right)_I , \tag{26}$$

where the isothermal reactivity response is defined consistent with equation (9),

$$\left(\frac{\Delta T}{\sqrt{T}}\right)_I = T'(\bar{P})\ \Delta\bar{P} \ /\ \sqrt{T}(\bar{P}) \ , \tag{27}$$

where $T'(P)$ is the derivative and P_α is the power in cell - α. The α-cell relative neutron production is defined,

$$\rho_{\alpha R} = \phi^1_{o\alpha}\ \phi^1_\alpha \rho_\alpha \ / \sum_\alpha \ \phi^1_{o\alpha}\ \phi^1_\alpha \rho_\alpha \ . \tag{28}$$

This expression may be simplified if the adjoint flux is approximated with the direct flux as suggested by Wade[17] and the direct perturbed flux is taken to be the initial steady-state solution. In this case,

$$\rho_{\alpha R} = (\phi^1_{o\alpha})^2 \rho_\alpha \ / \ \sum_\alpha \ (\phi^1_{o\alpha})^2 \rho_\alpha \ . \tag{29}$$

The first application of this result is to the spatial weighting due to the temperature distribution across a fuel assembly. In this case the cell consists of a HAMMER pin-cell, each fuel bearing cell is neutronically identical (i.e., all ρ_α are equal) and

$$\rho_{\alpha R} = (\phi^1_{o\alpha})^2 \ / \ \sum_\alpha \ (\phi^1_{o\alpha})^2 \ . \tag{30}$$

Using the TWOTRAN-II assembly flux distribution and corresponding pin-wise temperature distribution, the assembly spatial weight factor was determined

using equations (26) and (30).* Since the pin-wise fast flux is essentially flat across an assembly, all pins are weighted equally and S_T^{ass} was found to be $\lesssim 1.01$.†

It is noteworthy that in a typical BWR the fuel pins are not identical and some increase in Doppler feedback may result from the spatial weighting across an assembly.

Equation (29) may also be applied to the Doppler spatial weighting due to the core assembly-wise temperature distribution. The assembly fuel temperature is determined from the local power using equation (11) and the α-assembly reactivity response is

$$\Delta\rho_\alpha \propto \Delta T(P_\alpha) \,/\, \sqrt{T(P_\alpha)}. \tag{31}$$

The spatial weighting function (Equations (26) and (29)), $\phi_{o\alpha}{}^2 P_\alpha$, may be approximately represented as a function of power by assuming P_α to be constant and taking the fast flux to be proportional to the assembly power, i.e.,

$$(\phi_{o\alpha}^1)^2 P_\alpha \rightarrow P_\alpha{}^2 . \tag{32}$$

That the spatial behavior of the fast flux and power are similar can be derived from the two-group diffusion equations by neglecting leakage

---

*The power perturbation used in this case maintained the initial pin-wise power distribution. This is expected to be typical for most cases.

†Implicit in this argument is the separability of the assembly and core weight factors. This may be justified on the basis of the smallness of S_T^{ass}.

terms (which are small) and noting that the total fast cross section is essentially flat in space. For the RESAR-3 core the rms deviation of the left and right hand sides of Eq. (32) is $\sim$ 8%. S_T then becomes

$$S_T = \sum_{\alpha} \left(P_\alpha^2 / \sum_{\alpha'} P_{\alpha'}^2\right) \cdot \frac{\Delta T(P_\alpha)}{\sqrt{T(P_\alpha)}} \Big/ \left(\frac{\Delta T}{\sqrt{T}}\right)_I . \tag{33}$$

Using Eq. (11) the local reactivity may be expressed in terms of power,

$$\Delta\rho(P) \;\alpha\; \frac{\Delta T(P)}{\sqrt{T(P)}} = \frac{(b+2cP)\Delta P}{\sqrt{r+a+bP+cP^2}} \quad , \tag{34}$$

where r is a constant relating ^{o}F to ^{o}R. In adiabatic analyses the local power change is generally taken proportional to power, $\Delta P \alpha P$, so that the power distribution is maintained.* This is physically reasonable for most transients, however, in Appendix A the more general case in which ΔP is an arbitrary polynomial in P is treated. Here it will be assumed, $\Delta P \alpha P$ and the local reactivity is conveniently expressed,

$$\Delta\rho \;\alpha\; \frac{\Delta T(P)}{\sqrt{T(P)}} = -\gamma\,(1 - \lambda P)P \tag{35}$$

where λ is determined by a, b, c and r and for the RESAR-3 core $\lambda = .044$ $(KW/FT)^{-1}$.† γ is a constant of proportionality. Substituting Eq. (35)

---

*Except for small power redistributions due to feedback.

†That the power coefficient, $\frac{\partial\rho}{\partial P} = -(1-\lambda P)$, is to a good approximation linear in P, may be seen from Figure 8. This expression is valid for $P \lesssim 10$ KW/FT.

in Eq. (33),

$$S_T = \sum_{\alpha} \frac{(P_\alpha^3 - \lambda P_\alpha^4)/(1-\lambda\bar{P})\bar{P}}{\sum_{\alpha'} P_{\alpha'}^2} \tag{36}$$

Introducing the assembly-wise power frequency distribution, $f(P_i)$, the sum over assembly-cells may be converted to a sum over power P_i,

$$S_T = \frac{\sum_i f(P_i)(P_i^3-\lambda P_i^4)/(\bar{P}-\lambda\bar{P}^2)}{\sum_i f(P_i)P_i^2} \quad . \tag{37}$$

The spatial weight factor may now be expressed as a function of the moments of the power frequency distribution, f,

$$S_T = \frac{< \hat{P}^3 > - \lambda < \hat{P}^4 > \bar{P}}{< \hat{P}^2 > (< \hat{P} > -\lambda\bar{P})} \tag{38}$$

where for convenience the relative power $P = P/\bar{P}$ has been introduced. The moments of f are related to the relative variance, V, by,

$$\begin{aligned} < \hat{P}^2 > &= 1 + V \\ < \hat{P}^3 > &= 1 + 3V \\ < \hat{P}^4 > &= 1 + 6V \\ < \hat{P}^5 > &= 1 + 10V \end{aligned} \tag{39}$$

The third and fourth central moments of f are generally small and for simplicity have been neglected here.* Substituting equations (39) in equation (38) leads to,

$$S_T = 1 + \frac{V}{1+V} \cdot \frac{2-5\lambda\bar{P}}{(1-\lambda\bar{P})} \tag{40}$$

As expected, as V tends to zero all nodes in the core become identical ($f(P) \rightarrow \delta(P-\bar{P})$) and S_T approaches unity. The decrease in S_T with increasing core average power may be explained by noting the change in Doppler feedback per unit increment of power, $\Delta\rho/\Delta P$, decreases with power, i.e., $\lambda > 0$ in equation (37). Consequently, as the core average power increases the nodal powers occur on the flatter portion of the $\Delta\rho(P)$ curve (Figure 5) and, as a result, the Doppler weight factor decreases.

B. Results

1. Cell Doppler Coefficients

The neutronics model as described in Section III is based on HAMMER ENDF/B-IV pin-cell and TWOTRAN-II assembly-cell calculations. In Table IV the Doppler reactivity feedback coefficients from 800 ^{o}K to 1000 ^{o}K at the base conditions (Tm = 586 ^{o}F and C_B = 1000 ppm) are presented for the pin-cells at the three enrichments. The feedback is determined by the U-238 loading and is seen to be essentially independent of enrichment.

*In the case of a very strongly peaked and asymmetric power distribution the third and fourth moments become appreciable and must be taken into account.

In Table V the corresponding TWOTRAN-II assembly-cell Doppler feedback coefficients are presented for the various RESAR-3 fuel assemblies. The controlled assemblies (4 and 5) exhibit a slightly reduced feedback due to spectrum hardening and subsequent reduction in temperature dependence of the fast group absorption cross section.* The overall variation in Doppler feedback, however, is small ($\lesssim$ 5%) and the feedback coefficients can, to good approximation, be taken to be independent of assembly type. The TWOTRAN coefficients are reduced by $\sim$ 13% relative to the pin-cell coefficients due to the presence of water holes and reduction in the temperature dependence of the fast group removal cross section.

In order to determine the effect of local moderator temperature and boron concentration on the feedback, HAMMER sensitivity calculations were performed and in Table VI the results are presented. It is seen the boron concentration has a negligible effect and the magnitude of the Doppler coefficient is decreased by $\sim$ 7% as a result of an increased removal cross section at the reduced moderator temperature. The effect on the spatial weighting of this Doppler/moderator coupling has been evaluated assuming a typical overall moderator temperature variation of $\sim$ 80 ^{o}F and is found to be $\lesssim$ 1%.

*Most of the U-238 resonance absorption occurs at the low end of the fast group (70% below 80 eV.).

2. Doppler Spatial Weighting - S_T

Using the RESAR-3 PDQ7-II model S_T has been determined. The calculations were performed in planar geometry with a uniform moderator temperature of T_M = 586 ^oF, equilibrium xenon and a boron concentration of C_B = 1000 ppm. The Doppler fuel temperature perturbation was taken proportional to the power (except for a small T_F-feedback power redistribution).

S_T was taken as the ratio of the reactivity feedback in the temperature-distributed case to that for the isothermal case. Calculations were performed for a set of 8 control patterns including the all rods out (ARO) case, the two operating banks (C and D) inserted (BCDI) and 6 typical intermediate octant symmetric patterns described in Figure 6. (This set is believed to adequately cover the power distributions of interest.) Each control pattern was calculated at 108, 61 and 32 percent of rated power. The results of these calculations are presented in detail in Appendix C. In Figure 7 the resulting S_T's are plotted against the variance of the assembly power frequency distribution at 108, 61 and 32 percent power. In general, the data does not vary smoothly as a function of variance and this is believed to be due to numerical roundoff and to the effects of the higher moments of $f(P_i)$. S_T varies from unity in the isothermal (V = 0) case to 1.18 for a relatively broad V = .12 power distribution ($\sim$ 35% standard deviation) at 32% P_o.

For comparison, also included in Figure IV-2 is the analytic S_T result, equation (40), which is seen to be in good agreement with the

PDQ7-II numerical data. Both results approach unity as V tends to zero and are essentially linear for $V \lesssim .09$. The largest discrepancy occurring for 108% P_o at $V \sim .12$, results in a small, $\sim 1.5\%$, underprediction of core reactivity. It is concluded that Equation (40) provides a simple and accurate prescription for calculating S_T .

Additional PDQ7-II calculations were performed in order to determine the sensitivity of these results to (1) the particular RESAR-3 fuel assembly loading pattern and (2) the magnitude of the local Doppler feedback.* First, the planar checkerboard fuel assembly distribution was replaced by a uniform loading of 2.6 w/o fuel. Calculations of S_T for this uniform core were found to agree well with the analytic result determined using Equation (40). Also, calculations in which the Doppler feedback was increased uniformly across the core showed no effect on the value of S_T .

Finally, the effect of the rod heat-transfer calculation of the pin fuel temperature on S_T was evaluated as follows. In a simplified fuel rod model in which the heat is generated uniformly in the fuel meat, the steady-state temperature drop across the pellet and gap are,

$$\Delta T_{pellet} = \frac{P}{4\pi k_F}$$

$$\Delta T_{gap} = \frac{P}{2\pi k_G} \ln \frac{r_1}{r_2} \qquad (41)$$

*Note that the analytic model is independent of these variations.

where k_F (k_G) and r_2 (r_1) are the pellet (gap) conductivity (assumed to be constant) and outer radius respectively. The effective fuel pin temperature is,*

$$T_{eff} = T_M + \Delta T_{gap} + \frac{\omega}{2} \Delta T_{pellet} \tag{42}$$

where ω has been determined by Olhoeft[18] to be $\omega = .85$, to account for the preferential surface absorption. Taking the conductivities to be of the form,

$$k_F = k_{Fo} (1 + \mu P)^{-1} \quad (\mu > 0) \tag{43}$$

and

$$k_G = k_{Go} (1 - \nu P)^{-1}, \quad (\nu > 0)$$

T_{eff} may be expressed,

$$T_{eff} = T_M + \frac{1}{2\pi k_{Go}} \ln \frac{r_1}{r_2} + \frac{\omega}{8\pi k_{Fo}} P - \frac{\nu}{2\pi k_{Go}} \ln \frac{r_1}{r_2} + \mu \frac{\omega}{8\pi k_{Fo}} P^2 . \tag{44}$$

*The film and clad temperature drops are small and are neglected here.

The quantities, k_{Fo}, k_{Go}, μ and ν were determined from ΔT_{gap} and ΔT_{pellet} given in RESAR-3.[14]

In order to evaluate the effect of expected large operating uncertainties in the conductivities, (k_{Fo}, k_{Go}, μ,ν) were varied by 10% in the PDQ7-II calculations of S_T. These variations resulted in a negligible ($\lesssim$ .5%) change in S_T. It is important to note, however, that although the uncertainties in the thermal conductivities have a negligible effect on S_T, it is estimated they result in a 10-20% uncertainty in Doppler feedback due to fuel pin temperature uncertainty.

3. Vendor Comparisons

The Doppler reactivity coefficient calculated using PDQ7-II for the ARO core is compared to the RESAR-3 analysis in Table VII and Figure 8. The buckling contribution to the planar PDQ7-II results is separated out since it is a result of a predetermined temperature-dependent axial buckling which accounts for the effect of the axial fuel temperature distribution.

The Hellstrand correction accounts for the difference in the resonance integral calculation in the HAMMER and RESAR-3 pin-cell analysis; HAMMER uses the ENDF/B-IV data while the RESAR/LEOPARD determination is based on an empirical fit of the Hellstrand measurements or more accurate calculations.[19] A detailed comparison of these approaches has been made and the effect of these differences estimated to be $\sim$ 9% in Doppler coefficient.[1] When this renormalization is applied and consistent bucklings are used, the PDQ7-II and RESAR-3 results agree to within $\sim$ 4%.

With regard to the spatial weight factor, Sha[6] has made an empirical determination of S_T by fitting Doppler-only PWR power coefficient data for the Yankee, Saxton, BR-3 and Selni cores. He determined that ΔT_{pellet} should be increased by a factor of $\sim$ 1.57 to account for core spatial weighting. This increased temperature results in $\sim$ 20% increase in core effective temperature (^oF) and an $\sim$ 15% increase in core Doppler reactivity; $\Delta\rho^{eff} \sim \Delta T_{eff}/\sqrt{T}_{eff} = 1.15\ \overline{\Delta\rho}$. Poncelet[7] has evaluated S_T for Yankee-Core I using the steady-state fluxes determined from in-core activation measurements and equation (11). He finds S_T varies from 1.21 - 1.38 with rod pattern and that S_T decreases with core power.

Hellens et al.[20] performed 3-dimensional PDQ calculations and determined that S_T is close to 1.0 for operating cores.

In the present study it is found that S_T will vary between 1.0 and $\sim$ 1.35 for operating cores and the value in any specific case is determined by the power level ($\bar{P}$) and shape (V). During certain accident conditions, such as a rod ejection, the power distribution may become severely distorted, resulting in a large variance, and S_T may approach $S_T = 2.0$.

Since S_T depends on the amount of variability in the core power distribution, it is generally correlated to the global power peaking factor.[9,10,21] However, S_T is determined by the total variability of the power distribution, V, rather than the point value, P_{max}. In Figure 9 the correlation of S_T to P_{max} and V is compared for the cases evaluated in this study. This comparison indicates that correlating S_T to P_{max}, rather than V, introduces $\sim$ 5% additional uncertainty into the core Doppler feedback (assuming $S_T = 1.4$).

It is also important to note that the correlations of S_T (P_{max}) generally neglect the power level, $\bar{P}$, dependence and will therefore introduce additional uncertainty into S_T.

V. FLUX-DISTRIBUTION SPATIAL WEIGHTING - S_F

In practice the isothermal reactivity ρ_I is determined for a reference flux state, ϕ_1, rather than the actual operating state, ϕ_2. The effect of this simplification may be accounted for using the flux-dependent weighting factor, S_F. In order to determine the flux-dependence of the isothermal reactivity, equation (23) may be expanded as,

$$\Delta\rho_I(\phi,\bar{T}) = \frac{\sum_{\alpha,gg'} \phi^1_{o\alpha}\, \phi^1_{\alpha}\, \Delta\rho_\alpha P_{\alpha gg'}}{\sum_{\alpha,gg'} \phi^1_{o\alpha}\, \phi^1_{\alpha} P_{\alpha gg'}} . \tag{45}$$

Since all nodes receive the same temperature increment in the isothermal case and the local Doppler coefficient is independent of the spatial index-α (see Table IV and V), the local Doppler response, $\Delta\rho_\alpha$, is uniform across the core,* $\Delta\rho_\alpha = \overline{\Delta\rho}_{local}$. It then follows that,

$$\Delta\rho_I = \Delta\rho_{local}\,(\bar{T},\ \bar{T}_M,\ C_B) \tag{46}$$

and the isothermal reactivity is <u>independent</u> of the flux-distribution used in the reference calculation. It is important to note that the local reactivity $\Delta\rho_{local}$ is dependent on the core average fuel and moderator temperature and boron concentration.

---

*It is conceivable in an extreme accident situation that an assembly-wise moderator temperature variation of $\gtrsim$ 200 °F could result in a spatial variation in $\Delta\rho_\alpha$ and deviations from Eq. (46) of the order of $\gtrsim$ 5%.

That the isothermal reactivity, $\Delta\rho_I$, is independent of the flux distribution implies that the flux-distribution weight factor S_F is unity ($S_F = 1.0$). In order to demonstrate this, PDQ7-II calculations were performed for the 8 control patterns described in Figure 6 and in Table VIII the results are presented. It is concluded that $S_F = 1.0$.

Since the calculation of Doppler feedback may always be decomposed into (1) an isothermal reactivity calculation and (2) a temperature-distribution weight factor, the time dependent solution is only required for the determination of the weight factor, S_T (specifically, only the variance of the power distribution is required). The isothermal reactivity is determined by the core-average fuel and moderator temperature and boron concentration. (The dependence on T_M and C_B is weak and in many cases may be neglected without significant error.) In practice, therefore, the Doppler feedback in a transient analysis may be determined as follows,

1. Isothermal feedback determined from the Doppler coefficient, α, using the instantaneous values of ($\bar{T}$, $\bar{T}_M$, $\bar{C}_B$) as

$$\Delta\rho_I = \alpha(\bar{T}, \bar{T}_M, \bar{C}_B)\ \Delta\bar{T}, \tag{47}$$

2. S_T determined from equation (40) using the variance of the instantaneous power distribution, V(t).

VI. SUMMARY AND CONCLUSIONS

The focus of this evaluation has been the core Doppler weighting and, although there has been some emphasis on the PWR, most of the analysis may also be applicable to the BWR.

The isothermal reactivity is found to be independent of flux state and the flux-distribution weight factor, S_F, is unity.

The temperature-distribution weight factor, S_T, is found to vary from 1.0, for a high power and/or flat power distribution to $\sim$ 1.35 for a very broad (large variance) low power distribution. S_T is determined for operating states by a simple function of the core-average power and power distribution-variance. The derivation of this result is based on the assumption that the local reactivity weighting is P^2 and that the spatial dependence of the reactivity enters only through the local power, $P(\underline{x})$. This simplification is not possible for non-local feedbacks, e.g., moderator or void feedback, which are determined by the local power as well as the power at neighboring locations.

ACKNOWLEDGEMENT

The authors wish to thank Ellie Mitchell for her cheerful assistance and patience in interpreting and typing this manuscript.

References

1. M. Todosow, J. F. Carew, D. J. Diamond, "Evaluation of Temperature Dependent Resonance Integrals Using the HAMMER Code", BNL-NUREG-23500, Brookhaven National Laboratory (1977).

2. G. Lellouche, D. Diamond, M. Levine, "Application of Reactivity Weight Factors to Reactor Transients", BNL-16650, RP-1020, Brookhaven National Laboratory (1972).

3. W. H. Arnold and R. A. Dannels, "A Monte Carlo Study of the Doppler Effect in UO_2 Fuel", WCAP-1572, Westinghouse Electric Corp. (1960).

4. H. E. Jackson and J. E. Lynn, "Resonant Absorption of Neutrons by Crystals", Phys. Rev., 127, 461 (1962).

5. M. Edenius, "Studies of the Reactivity Temperature Coefficient in Light Water Reactors", AE-RF-76-3160, AB Atomenergi (1976).

6. W. T. Sha, "An Experimental Evaluation of the Power Coefficient in Slightly Enriched PWR Cores", WCAP-3269-40, Westinghouse Electric Corporation (1965).

7. C. G. Poncelet, "Analysis of the Reactivity Characteristics of Yankee Core-I", WCAP-6050, Westinghouse Electric Corporation (1963).

8. J. B. Yasinsky and A. F. Henry, "Some Numerical Experiments Concerning Space-Time Reactor Kinetics Behavior", Nucl. Sci. Eng., 22, 171 (1965).

9. R. J. French, et al., "Indian Point Unit-2 Rod Ejection Analysis", WCAP-2940, Westinghouse Electric Corporation (1966).

10. R. C. Stirn, "Generation of Void and Doppler Reactivity Feedback for Application to BWR Design", NEDO-20964, General Electric Co., December (1975).

11. W. Rothenstein, Y. Barhen, E. Taviv, "The Revised HAMMER Code", EPRI-NP-565, Electric Power Research Institute (1977).

12. K. D. Lathrop and F. W. Brinkley, "TWOTRAN-II: An Interfaced, Exportable Version of the TWOTRAN Code for Two-Dimensional Transport", LA-4848-MS, Los Alamos Scientific Laboratory (July 1973).

13. C. J. Pfeifer, "PDQ-7 Reference Manual II", WAPD-TM-947(L), Bettis Atomic Power Laboratory (1971).

14. "RESAR-3 Reference Safety Analysis Report", Westinghouse Nuclear Energy Systems (1973).

15. A. J. Buslik, D. Cacuci and A. Aronson, "Power Peaking During Load Following Using Westinghouse Constant Axial Offset Power-Distribution Control", BNL-NUREG-22477, Brookhaven National Laboratory (1977).

16. S. Altomare and R. F. Barry, "The TURTLE 24.0 Diffusion Depletion Code", WCAP-7758, Westinghouse Electric Corp. (June, 1968).

17. D. C. Wade, "An Approximation to the Adjoint Constructed From the Flux", Trans. Amer. Nucl. Soc., 11, 314 (1968).

18. J. E. Olhoeft, "Evaluation of Nuclear Effective Temperature in Thermal Power Reactor Fuel", Trans. Amer. Nucl. Soc., 13, 306 (1970).

19. L. E. Strawbridge, "Calculation of Lattice Parameters and Criticality for Uniform Water Moderated Lattices", WCAP-3269-25, (September 1963).

20. R. L. Hellens, C. O. Dechand, M. E. Congdon, "The Interpretation of Power Coefficients Measured in Operating Cores", Trans. Amer. Nucl. Soc., 12, 914 (1969).

21. D. H. Risher, Jr., "An Evaluation of the Rod Ejection Accident in Westinghouse Pressurized Water Reactors Using Spatial Kinetics Methods", WCAP-7588, Westinghouse Electric Corp. (December, 1971).

22. F. A. Holden, H. C. Wohlers and R. H. Reinhart, "Thermal Expansion of Uranium Dioxide", TID-5722.

23. R. F. Barry, "LEOPARD - A Spectrum Dependent Non-Spatial Depletion Code", WCAP-3269-26, Westinghouse Electric Corp. (September, 1963).

Table I

RESAR-3 Reactor Core and Fuel Description

Fuel Assemblies	
Number	193
Rod Array	17 x 17
Rods per Assembly	264
Rod Pitch, in.	0.496
Overall Transverse Dimensions, in.	8.426 x 8.426
Fuel Rods	
Outside Diameter, in.	0.374
Diameter Gap, in.	0.0065
Clad Thickness, in.	0.0225
Clad Material	Zircaloy - 4
Fuel Pellets	
Material	UO_2 Sintered
Density (percent of Theoretical)	95
Fuel Enrichments w/o	
Region 1	2.10
Region 2	2.60
Region 3	3.10
Diameter, in.	0.3225
Rod Cluster Control Assemblies	
Neutron Absorber	Ag-In-Cd
Diameter, in.	0.341
Density, lbs/in.^{3}	0.367
Clad Thickness, in.	0.0185
Burnable Poison Rods (First Core)	
Material	Borosilicate Glass
Outside Diameter, in.	0.381
Inner Tube, O.D., in.	0.1805
Boron Loading (w/o B_2O_3 in glass rod)	12.5
Core Average Linear Power, kW/ft	5.43

Table II

PDQ7-II/TWOTRAN-II Planar Reactivity Comparisons

	ARO		BDI		BCDI	
	PDQ-II	TWOTRAN-II*	PDQ7-II	TWOTRAN-II*	PDQ7-II	TWOTRAN-II*
$T_F = 727^oC$	.9952	.9928	.9835	.9804	.9737	.9708
$T_F = 527^oC$	.9996	.9974	.9878	.9850	.9781	.9753
$\Delta\rho/\Delta T(pcm/^oF)^\dagger$	-1.2253	-1.2842	-1.2119	-1.3003	-1.2525	-1.2847
$\delta(\Delta\rho)\%$	4.5		6.8		2.5	

ARO - All Rods Out

BDI - Bank D Inserted

BCDI - Bank C and D Inserted

*Part of this discrepancy is due to the convergence criteria used in TWOTRAN-II

$^\dagger pcm = 10^5 \ln \frac{k_2}{k_1}$

Table III

PDQ7-II/RESAR-3 Comparison of Critical Boron Concentration and Moderator Coefficient For the ARO Base State

	RESAR-3	PDQ7-II
C_B Critical Boron (ppm)	894	912
Moderator Coeff. (pcm/^oF)	-6.6	-8.5

Table IV

HAMMER (ENDF/B-IV) Pin-Cell Doppler Feedback Coefficients* vs. Enrichment

Enrichment (w/o)	$\Delta\rho/\Delta T$(pcm/^{o}F)
2.1	-1.475
2.6	-1.470
3.1	-1.467

*The coefficients calculated here are based on a 200^{o}C temperature interval and differ slightly from a point Doppler coefficient.

Table V

TWOTRAN-II Doppler Feedback Coefficients* for the RESAR-3 Fuel Assemblies

	Fuel Assembly	$\Delta\rho/\Delta T$(pcm/^{o}F)
1.	2.1 w/o, uncontrolled	-1.294
2.	2.6 w/o, uncontrolled	-1.287
3.	3.1 w/o, uncontrolled	-1.285
4.	2.1 w/o, controlled	-1.250
5.	2.6 w/o, controlled	-1.249
6.	2.6 w/o, 20 burnable poison pins	-1.309
7.	3.1 w/o, 20 burnable poison pins	-1.306
8.	2.6 w/o, 16 burnable poison pins	-1.307
9.	3.1 w/o, 12 burnable poison pins	-1.301
10.	3.1 w/o, 10 burnable poison pins	-1.294
11.	3.1 w/o, 9 burnable poison pins	-1.266

*The coefficients calculated here are based on a 200^{o}C temperature interval and differ slightly from a point Doppler coefficient.

Table VI

Sensitivity of Doppler Feedback to Moderator Temperature and Boron Concentration Perturbations

Case	$\Delta k/k/\Delta T$ pcm/ ^{o}F	% Variation
1. Base $T_M = 586^{o}F$, $C_B = 1000$ ppm	-1.4708	0.0
2. C_B Perturbation $T_M = 586^{o}F$, $C_B = 800$ ppm	-1.4769	- .41
3. T_M - Perturbation $T_M = 500^{o}F$, $C_B = 1000$ ppm	-1.3711	+6.78

Table VII

RESAR-3/PDQ7-II Power Coefficient Comparison

Doppler Only Power Coeff. (pcm/% P_o)	PDQ7-II	RESAR-3
$\Delta\rho$ (ENDF/B-IV, $B^2=0$)	- 8.04	
$\Delta\rho$ (Hellstrand, $B_Z^2=0$)	- 8.91	
$\Delta\rho$ (Hellstrand, $B_Z^2\neq0$)	-10.55	-10.89

Table VIII

Doppler Flux-Distribution Weight Factor - S_F

Calculated by PDQ7-II†

	S_F*		
Power (%)	108	61	32
STATE			
ARO	1.00	1.00	1.00
BCDI-1^o,2^+,3^o	1.00	1.00	.994
BCDI-2^o,3^+	.999	.995	.991
BCDI-2^o,2^+	.996	.996	.988
BCDI-3^o,3^+	1.002	1.003	.993
BCDI-2^o,3^o	.998	1.001	.992
BCDI-1^o	.998	.997	.990
BCDI	.998	.997	.990

†Since the flux variations were affected by varying the control pattern, an additional perturbation of $\Delta\rho(\underline{x})$ is introduced. However, since $\Delta\rho$ is insensitive to control this effect is estimated to be $\lesssim$ 1%.

*Defined relative to ARO state.

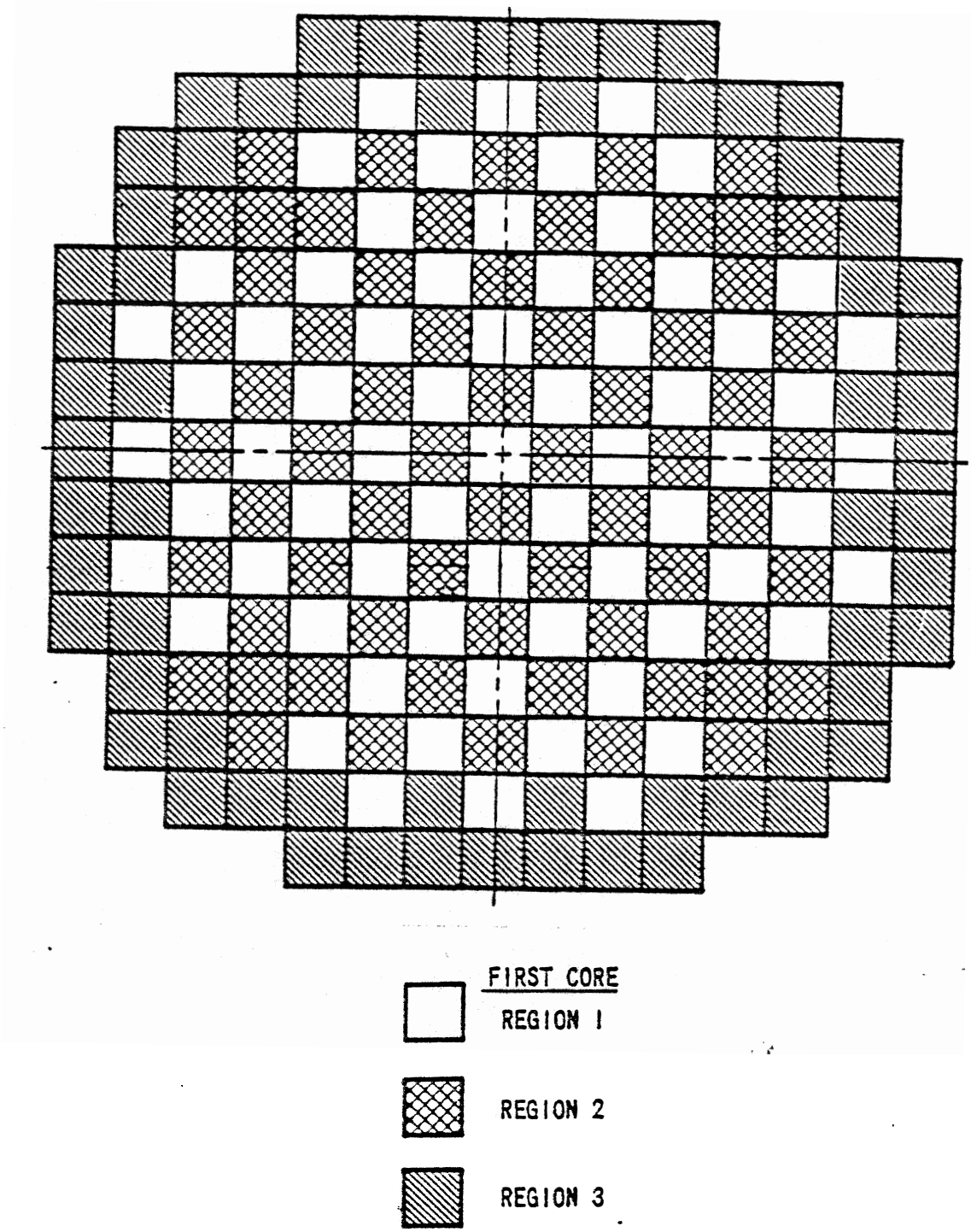

Fig. 1

Fuel Loading Arrangement

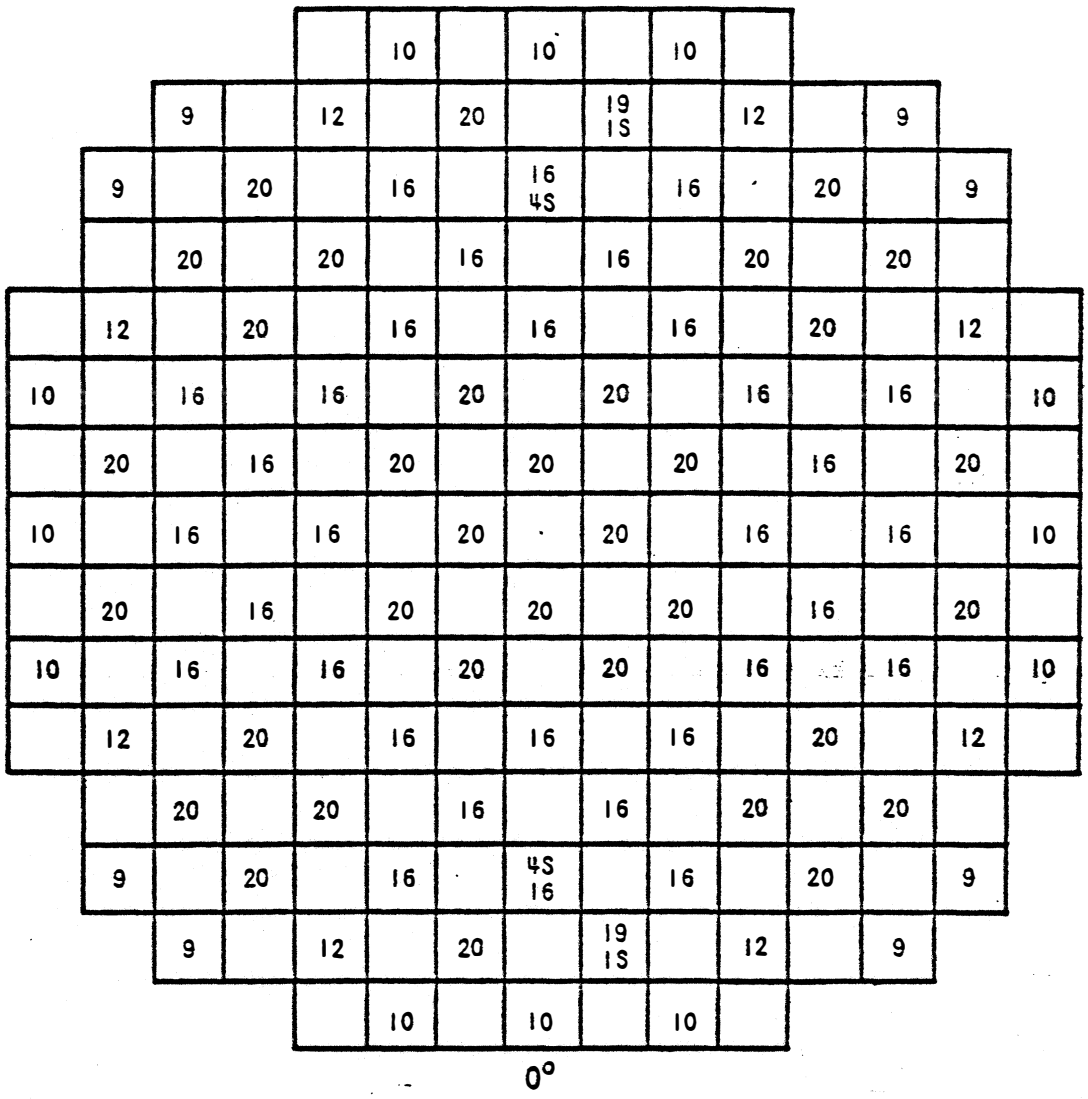

NUMBER INDICATES NUMBER OF BURNABLE POISON RODS
S INDICATES SOURCE ROD

Fig. 2

Burnable Poison Loading Pattern

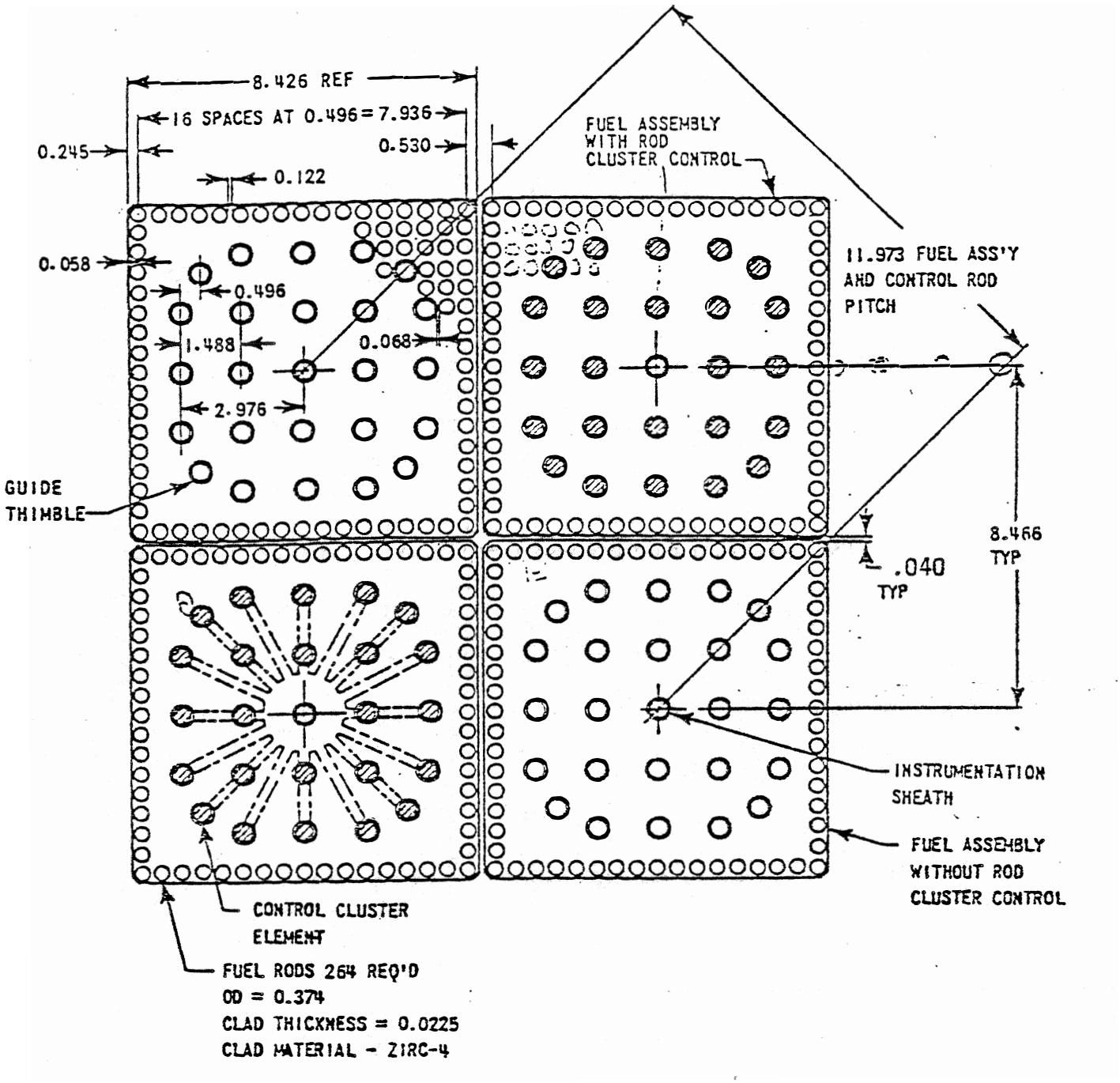

Fig. 3

Fuel Assembly Cross Section 17 x 17

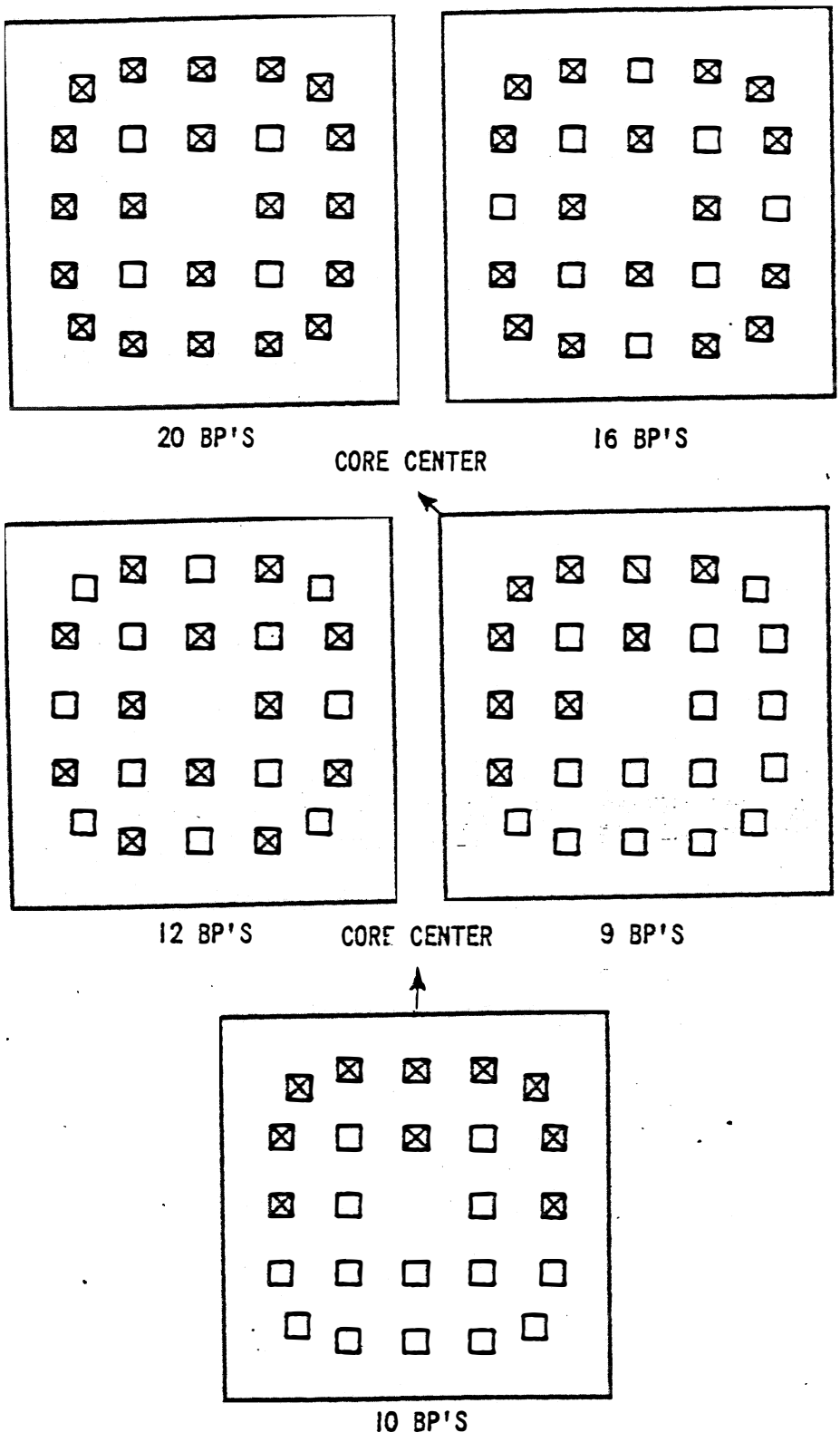

Fig. 4

Burnable Poison Rod Arrangement Within an Assembly

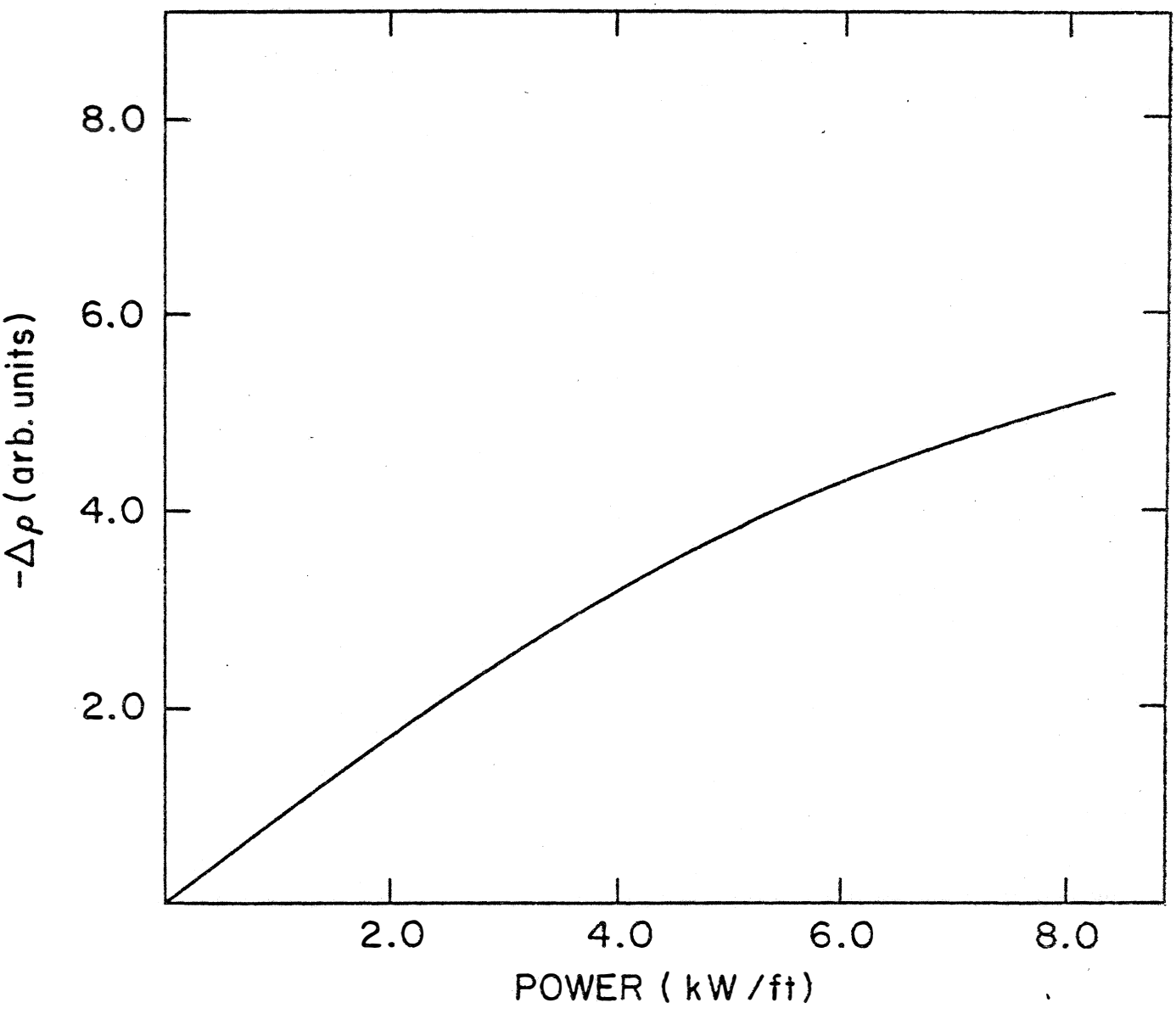

FIGURE 5. LOCAL DOPPLER REACTIVITY FEEDBACK VERSUS POWER ($\Delta P \propto P$)

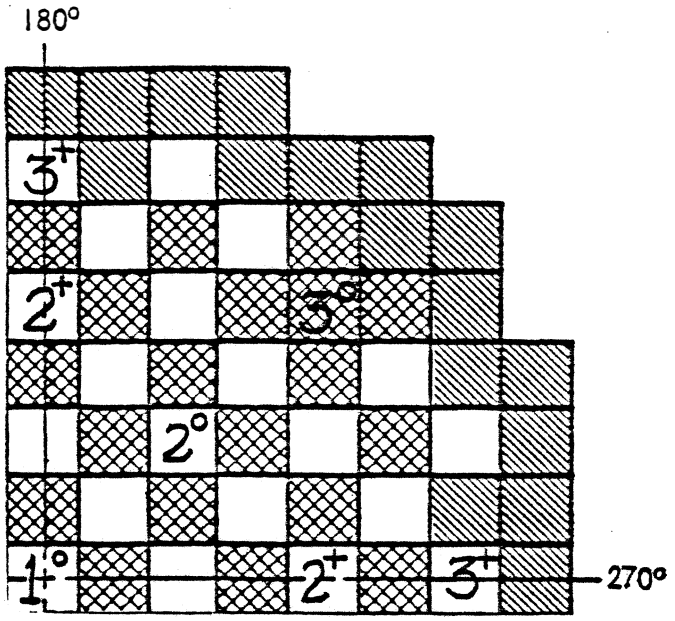

Control Patterns Calculated

BCDI

BCDI-1

BCDI-2^{o}, 3^{o}

BCDI-3^{o}, 3^{+}

BCDI-2^{o}, 2^{+}

BCDI-2^{o}, 3^{+}

BCDI-1^{o}, 2^{+}, 3^{o}

ARO

BCDI-N ≡ Bank C and D inserted and cluster N removed

ARO ≡ All clusters removed

Fig. 6

Rod Cluster Control Assembly (RCCA) Identification and Control Patterns Calculated

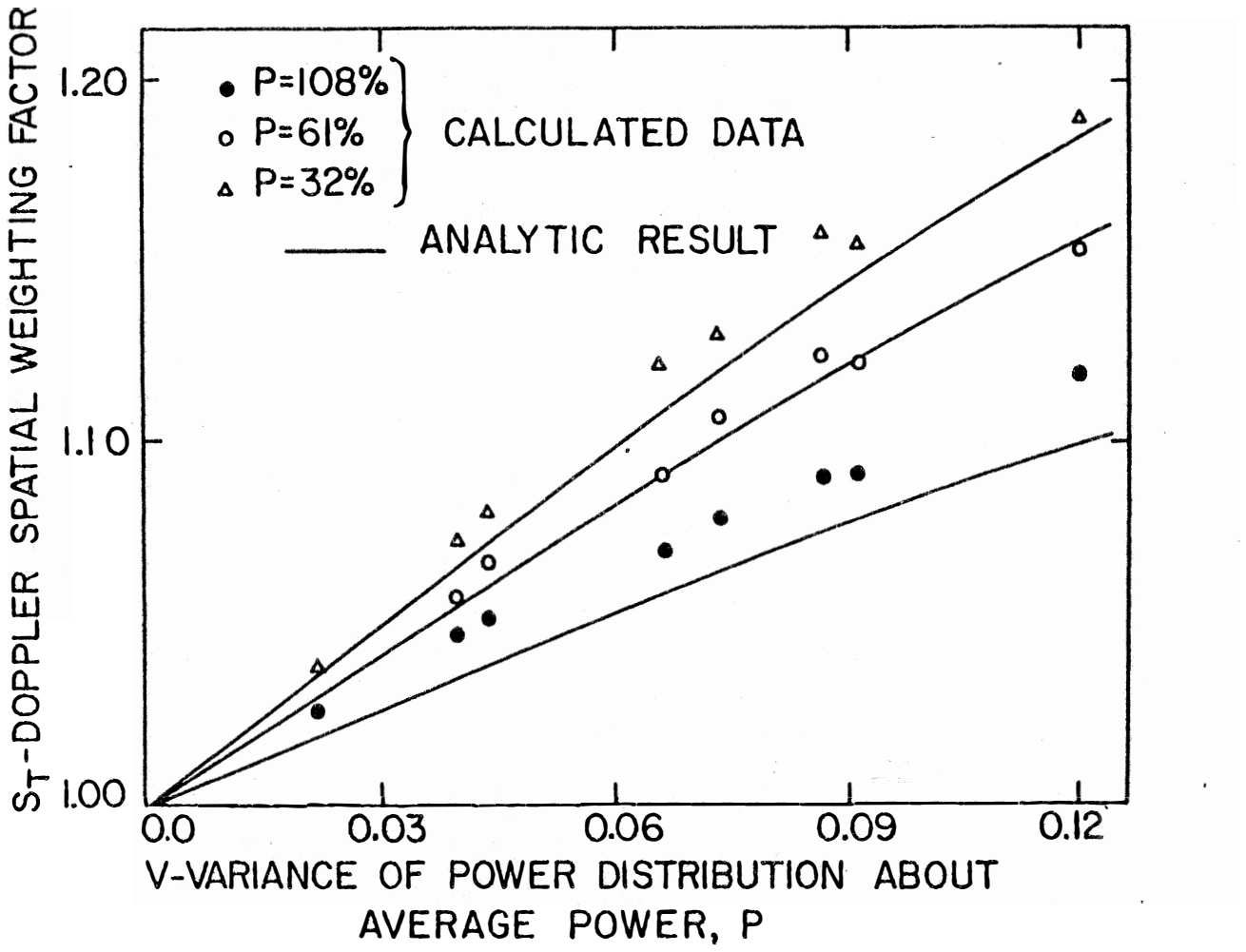

FIG 7 COMPARISON OF ANALYTIC AND PDQ7-II CALCULATED DOPPLER SPATIAL WEIGHTING FACTOR-S_T

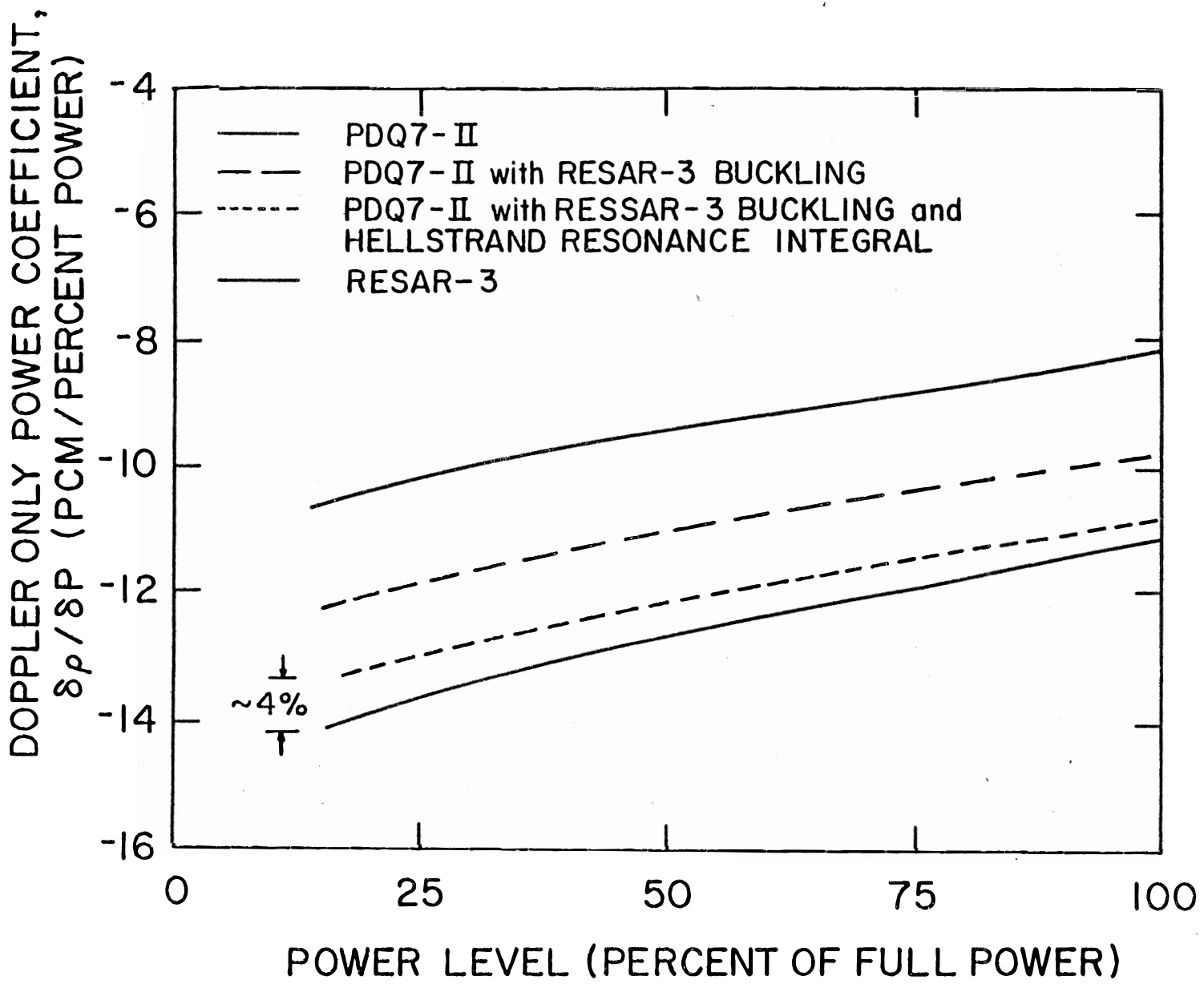

FIGURE 8. PDQ 7 and RESAR-3 DOPPLER ONLY POWER COEFFICIENT

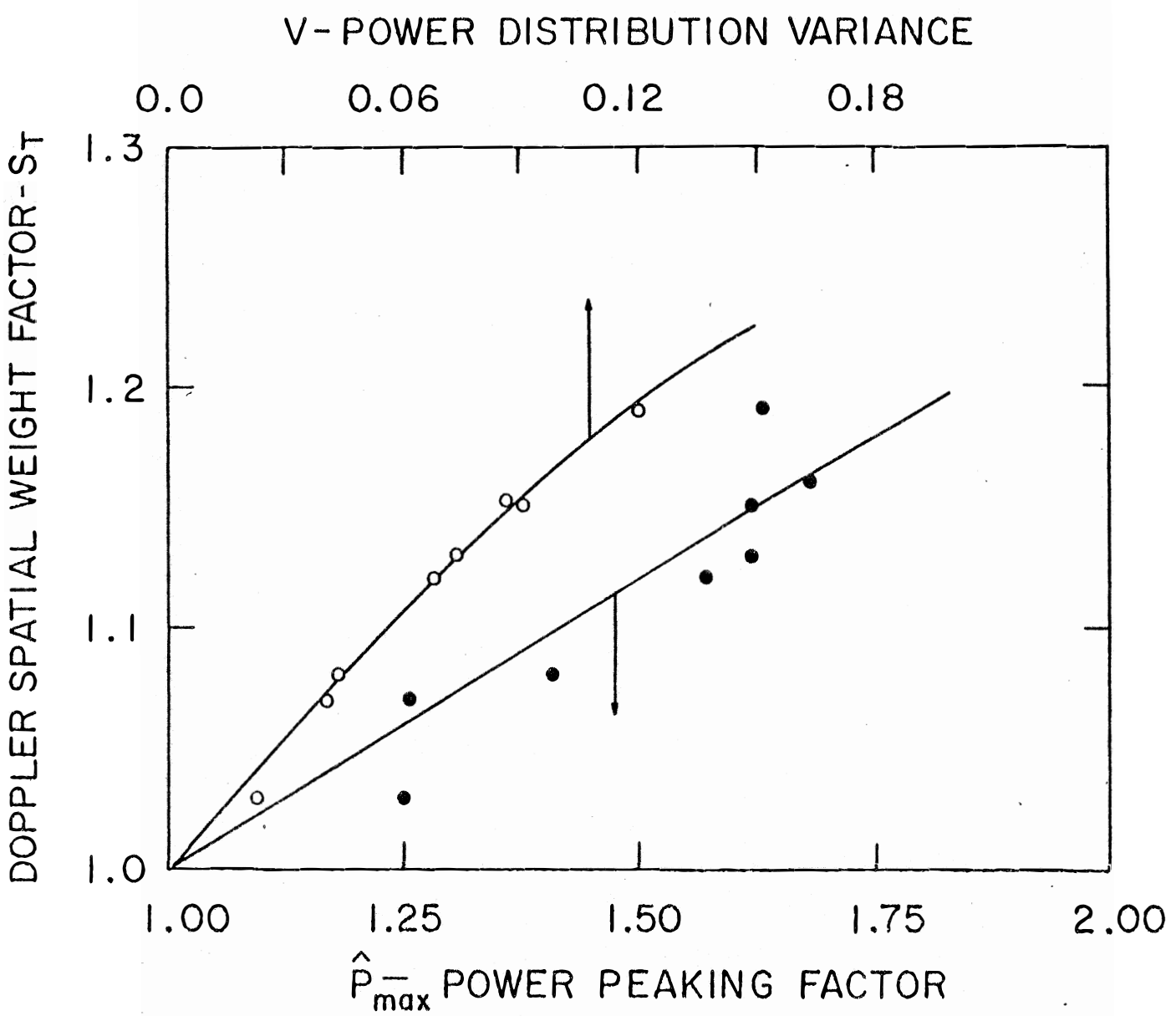

FIGURE 9. COMPARISON OF $S_T(\hat{P}_{max})$ AND $S_T(V)$ CORRELATIONS

Appendix A

Generalized Spatial Weight Factor-S_T

In typical adiabatic reactivity analyses the perturbation is assumed to be proportional to the power ($\Delta P \alpha P$) so the overall power distribution is preserved. In general, the power distribution is not maintained during a transient and the purpose of this appendix is to extend the analytic model for S_T (Equation (40)) to situations where ΔP is proportional to an arbitrary polynomial in power, i.e., $\Delta P \alpha P^n$.

Using Equation (34), S_T may be written,

$$S_T = \int f(P)dP \frac{P^2}{\langle P^2 \rangle} \frac{\Delta\rho(P)}{\Delta\rho(\bar{P})} \tag{A-1}$$

Assuming the local power change is proportional to P^n the local reactivity is,

$$\Delta\rho = \frac{\partial P}{\partial P} \Delta P = \gamma \, (-1+\lambda P) \, \Delta P$$

$$= - \gamma \, (1-\lambda P) P^n. \tag{A-2}$$

$$S_T = \frac{1}{\langle \hat{P}^2 \rangle} \cdot \frac{\langle \hat{P}^{n+2} \rangle - \lambda \langle \hat{P}^{n+3} \rangle}{(1 - \lambda\bar{P})} \bar{P} \tag{A-3}$$

Expressing the moments of $\hat{P}$ in terms of the variance, using Equations (39),* we find, for n = 0 (ΔP = constant),

$$S_T = 1 - \frac{V}{1+V} \frac{2\lambda\bar{P}}{1-\lambda\bar{P}} , \tag{A-4}$$

for n = 1 ($\Delta P \alpha P$)

$$S_T = 1 + \frac{V}{1+V} \cdot \frac{2-5\lambda\bar{P}}{1-\lambda\bar{P}} \tag{A-5}$$

and for n = 2 ($\Delta P \alpha P^2$)

$$S_T = 1 + \frac{V}{1+V} \cdot \frac{5-9\lambda P}{1-\lambda P} . \tag{A-6}$$

In all cases S_T approaches unity in the isothermal limit, $V \to 0$. In the n = 1 and n = 2 cases there is positive correlation between the spatial weighting ($\sim P^2$) and the feedback ($\Delta P \sim P^n$), with the high powered, high weight nodes receiving the largest power increment and feedback, and $S_T > 1.0$. In the n = 0 case (ΔP = constant) all nodes receive the same power increment and, due to the saturation of the Doppler feedback at high temperatures,† the high powered nodes receive the least feedback. Consequently, in this case there is negative correlation and $S_T < 1.0$.

---

*Which neglects the higher central moments of f(P) which are generally small.

†The saturation of the Doppler feedback at high temperatures results from the resonance broadening and decrease in self-shielding ($1/\sqrt{T}$ behavior) and, to a lesser extent, from the increase in gap conductance at elevated temperatures.

In Figure A-1 S_T is plotted for these three cases and, as expected, S_T is largest in the $\Delta P = P^2$ case where the correlation of feedback and weighting is strongest. This case corresponds to the later stages of a rod ejection accident where a significant power peak has developed. For a uniform perturbation, S_T-1 is small and negative.

The extension of this technique to higher order polynomials is straightforward.

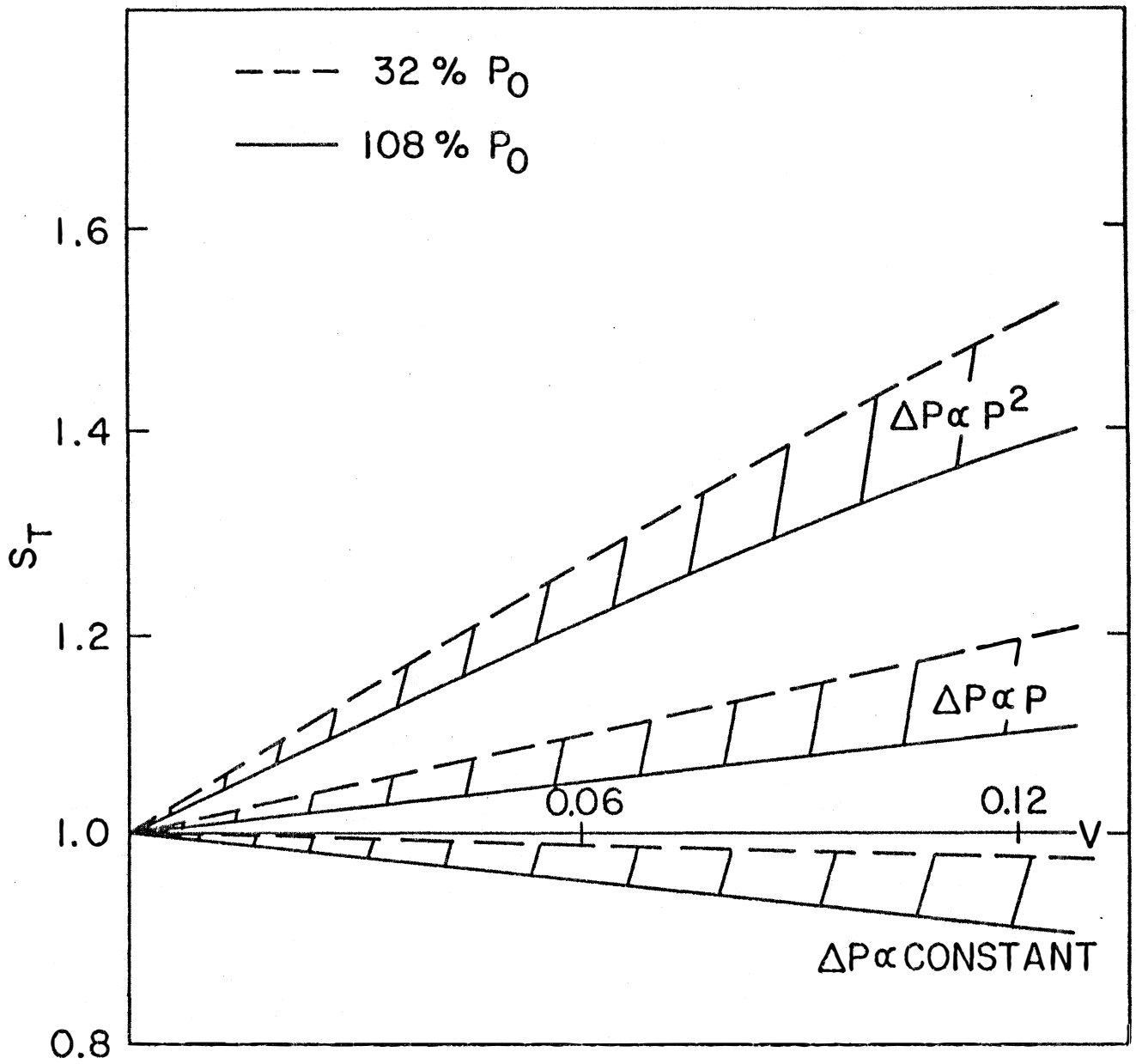

FIGURE A-1. $S_T(V)$ FOR SELECTED POWER PERTURBATIONS

Appendix B

HAMMER Sensitivity Evaluation

A number of calculations have been performed to examine the sensitivity of the Doppler coefficient to 1) changes in buckling, 2) inclusion or neglect of thermal expansion, and 3) the use of "resonance effective fuel temperatures", rather than volume averaged. An infinite reactor composed of a uniform array of specified fuel pin-cells was considered.

The HAMMER spectrum code was used in this study. A 2.6 w/o fuel pin-cell was constructed, based upon information for the Westinghouse RESAR-3[13] core. The important characteristics of the cell are summarized in Table I.

The moderator-coolant is light water at a pressure of 2250 psia, a temperature of 590 ^{o}F (core average), and contains 1190 ppm of dissolved boron.

The average fuel temperature at Beginning of Life (BOL) for the given linear power is 1283 ^{o}F. The average clad temperature at the core midplane at BOL is 662 ^{o}F.

HAMMER calculations were run with all parameters as described, for a buckling of 1.0×10^{-5} m^{-2}, with uniform fuel temperatures of 1233, 1283 and 1333 ^{o}F. The resultant infinite reactor eigenvalues and Doppler coefficient at full power are given in Table B-1. The infinite reactor

eigenvalue is k_∞ , while k_{eff} is the eigenvalue evaluated at the input buckling. (For this case the two are equal as a result of the low value for B^2.)

We next consider the effect of radial thermal expansion of the pellet, the clad, and the lattice pitch upon the Doppler coefficient. The pellet was expanded according to the relationship given in Reference 22. The clad was expanded using the coefficient of linear expansion for Zircaloy-2 from the LEOPARD manual.[23] The lattice was expanded by assuming that the coefficient of linear expansion for the grid spacers, which are made of Inconnel 718, is the same as that for stainless steel, and that T(grid) = T(mod). All densities, except that of the moderator, were adjusted appropriately. It should be noted that HAMMER, unlike a number of other spectrum codes, has no provision for an "extra region" to account for non-pin-cell core constituents such as the grid spacers, guide tubes, etc., and does not do thermal expansion internally.

The results of this calculation are presented in Table B-2. It may be noted that k_{eff} (= k_∞) increases slightly, while the Doppler coefficient increases by $\sim$ 1.5%, when compared to the results presented in Table B-1.

We now turn to the problem of incorporating some estimate for the leakage that is present in the finite reactor, into the infinite reactor calculation performed by HAMMER. (It should be noted that all succeeding cases incorporate any earlier changes, therefore, this calculation accounts for the changes due to thermal expansion also). To this end,

we input a value for the buckling that is based upon the core total geometric buckling.

$$B^2 = \left[\frac{2.405}{(2.54)(\frac{132.7}{2}) + 5.6}\right]^2 + \left[\frac{\pi}{(144)(2.54) + 2(5.6)}\right]^2 \text{ cm}^{-2} \qquad \text{(B-1)}$$

where the equivalent diameter of the core, 132.7 in., and the active core height, 144 in., are from the RESAR-3, and 5.6 cm is an estimate for the axial and radial reflector savings, which are assumed to be equal for this calculation.

The results of this calculation are presented in Table B-3, where now both k_∞ (evaluated at $B^2 \approx 0$) and k_{eff} (evaluated at the input core average buckling of 2.60216 m^{-2}) are given.

As compared to the previous case (Table B-2) the magnitude of the Doppler coefficient based upon k_∞ is seen to increase slightly ($\sim$ 0.7%), while the Doppler coefficient based upon k_{eff} is unchanged. Comparison of the k_∞ and k_{eff} values presented in Table B-3 shows the effect of the increased leakage due to the use of the core average buckling, while comparison of the k_∞ values of Tables B-2 and B-3 shows the effect of the different flux spectra and group constants (which are used in the evaluation of the eigenvalues).

As has been noted, in the calculation the fuel temperature is flat throughout the pellet. Physically this is clearly incorrect. The concept of "effective fuel temperature", or "resonance temperature" has been in use for some time to account for the effect of the constant temperature approximation on the calculated resonance escape probability.

By definition, the "effective fuel temperature" is that uniform temperature which will lead to the same resonance escape probability as that resulting from the actual distribution. A correlation based upon Monte Carlo calculations has been used in this study[18]:

$$T_{eff} = 0.85\ \bar{T} + (1 - 0.85)\ T_s \qquad \text{(B-2)}$$

where T_s and $\bar{T}$ are the surface- and volume-averaged temperatures, respectively, of a cylindrical fuel pin. Using a pellet surface temperature of 957 ^{o}F, the resulting effective fuel temperature at full power is found to be 1234 ^{o}F, a decrease of 49 ^{o}F.

We now incorporate this effect in the following way: taking the pellet dimensions and densities consistent with the appropriate volume-averaged temperature, we use T_{eff} for the Doppler broadening calculation only, assuming that in the neighborhood of full power that we are considering

$$T_{eff} = T_{av} - 49\ (^{o}F) \qquad \text{(B-3)}$$

The results from this calculation are presented in Table B-4 where again k_∞ and k_{eff} based values for the Doppler coefficient are given.

The net effect of this final adjustment has been to slightly increase the magnitude of the Doppler coefficients over the values presented in Table B-3.

Table B-1

Nominal Case - Full Power

T_f (°F)†	$k_\infty = k_{eff}$	Doppler Coeff. (pcm/°F)*	
1233	1.111373	-1.47	-1.45
1283	1.110559	-1.44	
1333	1.109759		

*pcm $\equiv \Delta\rho \times 10^{+5}$, where the reactivity is defined by $\Delta\rho = \ell n \frac{k_1}{k_2}$.

†T_f is the fuel temperature.

Table B-2

Effect of Thermal Expansion at Full Power

T_f (°F)	$k_\infty = k_{eff}$	Doppler Coeff. (pcm/°F)	
1233	1.111714	-1.48	-1.47
1283	1.110889	-1.46	
1333	1.110078		

Table B-3

Effect of Buckling at Full Power

T_f (°F)	k_∞	k_{eff}
1233	1.111263	1.094846
1283	1.110437	1.094034
1333	1.109625	1.093236
Doppler Coeff. (pcm/°F)	-1.48	-1.47

Table B-4

Effect of Use of Effective Fuel Temperature

at Full Power

T_f (^oF)	k_∞	k_{eff}
1184	1.112045	1.095614
1234	1.111218	1.094801
1284	1.110394	1.093992
Doppler Coeff. (pcm/^oF)	-1.49	-1.48

Appendix C

Detailed RESAR-3 PDQ7-II Doppler Feedback and Spatial Weighting Results

Table C-1

Isothermal and Temperature-Distributed RESAR-3 PDQ7-II

Doppler Feedback and Spatial Weight Factors

For the BCDI Base Conditions

$\bar{P}$(kw/ft)	5.7268	5.9948	3.2421	3.3939	1.6290	1.7919
%ΔP	4.936		2.795		3.000	
k^{I*}	.974270	.973894	.977982	.977742	.980657	.980376
Δk^{I}(pcm)	-38.60		-24.54		-28.66	
k^{D*}	.972964	.972554	.977079	.976810	.980126	.979802
Δk^{D}(pcm)	-42.15		-27.54		-33.06	
S_T	1.092		1.122		1.154	

*k^{I}(k^{D}) - isothermal (distributed-temperature) eigenvalue.

Table C-2

Isothermal and Temperature-Distributed RESAR-3 PDQ7-II

Doppler Feedback and Spatial Weight Factors

For the BCDI-1^{o} Base Conditions

$\bar{P}$(kw/ft)	5.7268	5.9948	3.2421	3.3939	1.6290	1.7919
R^I	.974651	.974275	.978365	.978125	.981041	.980760
Δk^I(pcm)	-38.59		-24.53		-28.65	
k^D	.973645	.973243	.977664	.977402	.980627	.980312
Δk^D(pcm)	-41.30		-26.80		-32.13	
S_T	1.070		1.092		1.122	

Table C-3

Isothermal and Temperature-Distributed RESAR-3 PDQ7-II

Doppler Feedback and Spatial Weight Factors

For the BCDI-2°, 3° Base Conditions

$\bar{P}$(kw/ft)	5.7268	5.9948	3.2421	3.3939	1.6290	1.7919
k^I	.986949	.986568	.990721	.990477	.993438	.993153
Δk^I (pcm)	-38.61		-24.63		-28.69	
k^D	.985610	.985194	.989791	.989517	.992889	.992559
Δk^D (pcm)	-42.22		-27.69		-33.24	
S_T	1.093		1.124		1.159	

Table C-4

Isothermal and Temperature-Distributed RESAR-3 PDQ7-II

Doppler Feedback and Spatial Weight Factors

For the BCDI-3^{o}, 3^{+} Base Conditions

$\bar{P}$(kw/ft)	5.7268	5.9948	3.2421	3.3939	1.6290	1.7919
k^{I}	.988675	.988292	.992454	.992209	.995177	.994891
Δk^{I} (pcm)	-38.75		-24.69		-28.74	
k^{D}	.987048	.986620	.991349	.991067	.994537	.994197
Δk^{D} (pcm)	-43.37		-28.45		-34.19	
S_T	1.119		1.152		1.190	

Table C-5

Isothermal and Temperature-Distributed RESAR-3 PDQ7-II

Doppler Feedback and Spatial Weight Factors

For the BCDI-2^{o}, 2^{+} Base Conditions

$\bar{P}$(kw/ft)	5.7268	5.9948	3.2421	3.3939	1.6290	1.7919
k^{I}	.983827	.983448	.987575	.987333	.990276	.989993
Δk^{I}(pcm)	-38.53		-24.51		-28.58	
k^{D}	.983236	.982839	.987181	.986925	.990050	.989747
Δk^{D}(pcm)	-40.39		-25.94		-30.61	
S_{T}	1.048		1.058		1.071	

Table C-6

Isothermal and Temperature-Distributed RESAR-3 PDQ7-II

Doppler Feedback and Spatial Weight Factors

For the BCDI-2^{o}, 3^{+} Base Conditions

$\bar{P}$(kw/ft)	5.7268	5.9948	3.2421	3.3939	1.6290	1.7919
k^{I}	.983984	.983604	.987736	.987494	.990440	.990156
Δk^{I}(pcm)	-38.63		-24.50		-28.68	
k^{D}	.983306	.982907	.987272	.987014	.990169	.989862
Δk^{D}(pcm)	-40.59		-26.14		-31.01	
S_{T}	1.051		1.067		1.081	

Table C-7

Isothermal and Temperature-Distributed RESAR-3 PDQ7-II

Doppler Feedback and Spatial Weight Factors

For the BCDI-1^{o}, 2^{+}, 3^{o} Base Conditions

$\bar{P}$(kw/ft)	5.7268	5.9948	3.2421	3.3939	1.6290	1.7919
k^{I}	.987601	.987219	.991374	.991130	.994093	.993807
Δk^{I}(pcm)	-38.69		-24.62		-28.77	
k^{D}	.986451	.986039	.990575	.990305	.993620	.993297
Δk^{D}(pcm)	-41.78		-27.26		-32.51	
S_T	1.080		1.108		1.130	

Table C-8

Isothermal and Temperature-Distributed RESAR-3 PDQ7-II

Doppler Feedback and Spatial Weight Factors

For the ARO Base Conditions

$\bar{P}$(kw/ft)	5.7268	5.9948	3.2421	3.3939	1.6290	1.7919
k^I	.995724	.995339	.999527	.999281	1.00227	1.00798
Δk^I(pcm)	-38.66		-24.60		-28.74	
k^D	.995355	.994960	.999282	.999027	1.00213	1.00783
Δk^D(pcm)	-39.77		-25.47		-29.95	
S_T	1.029		1.035		1.042	

Distribution List

M. Dunenfeld, NRC (5)
D. Fieno, NRC
S. Weiss, NRC (8)
RCSAG, BNL (9)
RSP Group Leaders, Division Heads, BNL (13)
W. Kato, BNL
H. Kouts, BNL
P. Check, NRC
R. Baer, NRC
D. Ross, NRC
D. Eisenhut, NRC
R. Mattson, NRC
V. Stello, NRC
W. Minners, NRC
J. Telford, NRC
L. Tong, NRC
T. Murley, NRC
S. Hanauer, NRC
NRC Public Document Room
NRC Bethesda Technical Library
B. Zolotar, EPRI
G. Sherwood, GE
C. Eicheldinger, W
F. Stern, C-E
J. Taylor, B & W
W. Nechadon, Exxon
J. Rahmstahler, INEL
R. Brodsky, DOE
ACRS, NRC (15)
F. Coffman, NRC
C. Berlinger, NRC
M. Fleishman, NRC
H. Richings, NRC
A. Buslik, BNL
J. Christenson, U. Cinn.
A. Schor, MIT
V. Demasi, GPU
Z. Rosztoczy, NRC
A. McFarlane, W
S. Lane, BNL